MODELING LONGITUDINAL DYNAMICS IN THE FERMILAB BOOSTER SYNCHROTRON*

J.-F. Ostiguy†, V. Lebedev, C.M. Bhat
Fermilab, Batavia, IL, USA

Abstract

The PIP-II project will replace the existing 400 MeV linac with a new, CW-capable, 800 MeV superconducting one. With respect to current operations, a 50% increase in beam intensity in the rapid cycling Booster synchrotron is expected. Booster batches are combined in the Recycler ring; this process limits the allowed longitudinal emittance of the extracted Booster beam. To suppress eddy currents, the Booster has no beam pipe; magnets are evacuated, exposing the beam to core laminations and this has a substantial impact on the longitudinal impedance. Noticeable longitudinal emittance growth is already observed at transition crossing. Operation at higher intensity will likely necessitate mitigation measures. We describe systematic efforts to construct a predictive model for current operating conditions. A longitudinal only code including a laminated wall impedance model, space charge effects, and feedback loops is developed. Parameter validation is performed using detailed measurements of relevant beam, rf and control parameters. An attempt is made to benchmark the code at operationally favorable machine settings.

INTRODUCTION

Proton Improvement Plan-II [1] (PIP-II) is Fermilab's plan for delivering higher intensity proton beams in support of intensity frontier physics and provide a flexible platform for further enhancements of its accelerator complex. The centerpiece is a new 800-MeV superconducting linear accelerator (SCL) which will supply beam to the Booster synchrotron, replacing the existing warm 400 MeV linac. The increased energy will reduce the space charge tune shift in this machine by 30%, and allow for an increase in intensity on the order of 50%. It is assumed that this can be realized while keeping beam losses at the present level. Concretely, this implies not only that uncontrolled losses in the Booster itself need to remain at the current level (0.5 kW) but also that the longitudinal emittance at ejection should not be degraded beyond its current value (0.1 eV-s, 100%). The limit is set by the slip-stacking scheme employed in the downstream machine (Recycler). Simulations are needed to help assess to what extent this objective can be attained.

BOOSTER SYNCHROTRON

The Booster synchrotron is a 15 Hz rapid cycling machine. Its combined function bending magnets are powered by a resonant circuit that produces a sinusoidal field ramp. Twenty rf stations (originally 16) deliver a maximum 1.2 MV total ring voltage. The linac (H^-) beam is accumulated during multiple turns (10 to 18), adiabatically captured and accelerated to 8 GeV. Transition takes place at (γ_t = 5.45). A distinctive feature of the machine is that the bending magnets do not have a conventional vacuum chamber. To circumvent issues with eddy currents that arise with a conventional chamber, the volume between the magnet poles is evacuated and the beam is directly exposed to the pole laminations. While this configuration is cost-effective, it also results in unusually large reactive and resistive contributions to the ring impedance. The Booster is currently operated without a formal γ_t jump system. A system using dedicated pulsed quadrupoles was installed in the late 1980's but was later decommissioned due to problems with orbit steering and envelope perturbations.

Wall Impedance

Clearly, credible simulations demand a reasonable model of the magnet wall impedance. Over the years, a succession of increasingly refined analytical models were devised. The magnet impedance was also measured in 1986 and in 2001 using a wire technique to simulate the beam [2]. We settled on an analytical expression for rectangular symmetry obtained a few years ago by Burov and Lebedev and independently by Macridin. The details are too cumbersome to reproduce here; the interested reader can consult the references [3, 4]. With careful adjustment of geometric parameters and experimentally obtained information about high-frequency dependence of the lamination material permeability, satisfactory agreement with wire measurements is obtained. Even though it assumes an idealized periodic geometry, the analytical expression provides an impedance model that (1) is consistent with causality and (2) reflects the essential physics. Figure 1 shows the relative contri-

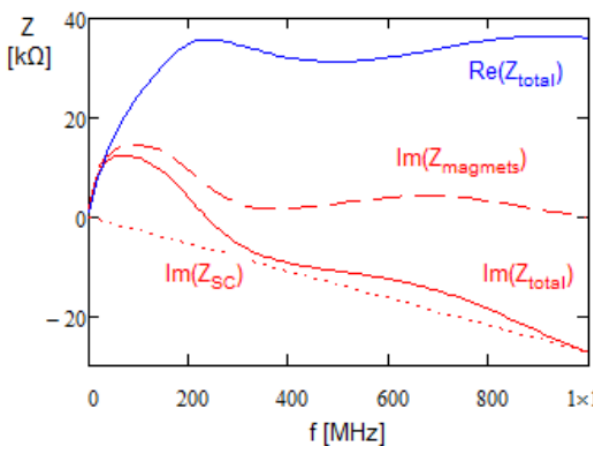

Figure 1: Machine impedance at transition. The total imaginary component is dominated by space charge.

* Work performed for Fermi Research Alliance, LLC under Contract No. DE-AC02-07CH11359 with the United States Department of Energy
† ostiguy@fnal.gov

ISBN 978-3-95450-147-2

butions of the wall impedance computed from the model (which is weakly dependent on energy) and the space charge impedance at transition.

RF Program

For the simulations, we opted to use as input, an rf program representative of actual operating conditions. A typical rf voltage amplitude curve used in operations is shown in Fig. 2. The curve reflects some empirical optimization to minimize losses and emittance blow-up. The dip near transition suggests an attempt at mitigating the focusing asymmetry across transition. The latter is related to the fact that while the rf focusing is kept positive across transition, the impedance force (possibly dominated by space charge) changes sign. The mismatch triggers oscillations of quadrupole and higher order that filament, resulting in an increase in emittance. While the control system provides us-

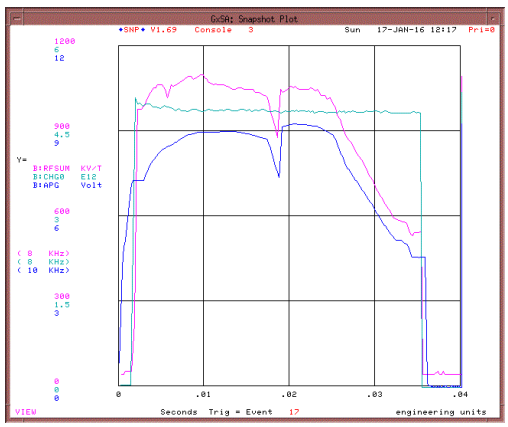

Figure 2: Cyan trace (RFSUM): RF voltage readback for a Booster cycle. The RFSUM signal is the vector sum of all rf stations voltages.

able rf voltage amplitude information, the corresponding rf phase information is not clean, especially around transition. Using a fast digital oscilloscope, raw signals were acquired for the cavity voltage sum (RFSUM), a resistive wall current monitor (RWM) and the radial position RFPOS. Data sets for beam intensities corresponding to 4,8,12 and 15 turns were obtained. Each set comprised two groups of 3.5 ms worth of samples (0.8 ns) one beginning at injection and the other centered around transition. Using data reduction techniques, the time delay between the rf zero crossing and the bunch arrival time were used to extract phase information through transition. Figure 3 shows that the rf phase undergoes rapid changes in the vicinity of transition; over approximately 10 turns, the phase is decelerating. The deceleration causes a dip in beam energy clearly visible in the RPOS signal.

SIMULATIONS

Code

A number of codes to simulate longitudinal dynamics in proton synchrotrons are available. Some representative examples include ESME, LONG1D, and Longitudinal HEAD-

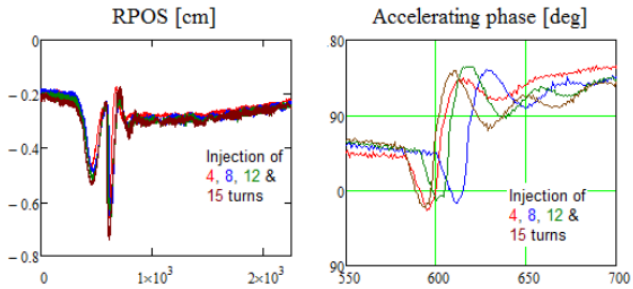

Figure 3: Measured radial position (left) and rf phase (right) vs turn number across transition. The data starts approximately 1.75 ms before transition (corresponding to turn 0 on these plots).

TAIL (CERN); however, these codes are designed to be applicable to a range of problems and their internals are complex. In the context of this work, it was decided that the best course of action would be to start with a minimalist and narrowly focused code that can be controlled fully. The tracking engine was implemented in C; it is supplemented with MathCAD sheets for analysis and plotting. Tracking is based on a difference mapping

$$\begin{aligned} \phi_{n+1} &= \phi_n + \left(\frac{\omega_{0,n+1}}{\omega_{0,n}}\phi_n - \phi_{s,n}\right) + 2\pi h\eta\frac{\Delta E_n}{\beta^2 E} \\ \Delta E_{n+1} &= \Delta E_n + eV_0[\sin(\phi_n) - E_{s,n}] - V_b(\phi) \end{aligned}$$

where $\Delta E = (E - E_{s,n})$ is the deviation from the synchronous energy $E_{s,n}$ at turn n, ω_0 is the revolution frequency ϕ_s is the rf phase and η is the phase slip factor. V_0 is the sum of all cavity voltages and V_b represents the beam induced voltage integrated along the machine circumference and the harmonic factor $h = 84$. This "lumped" approximation is justified when the synchrotron tune ν_s is low (for the Fermilab Booster, $0.1 < \nu_s < 0.001$) i.e. when no significant evolution of the phase space takes place on the scale of a turn. Only one bunch is tracked; the beam is assumed to have periodicity T/h. This implies that coupled bunch motion is not included. In the Booster, this motion is well supressed by an active damping system.

At every turn, particles are propagated using the phase mapping. The beam current is then obtained by projecting the distribution, Fourier transformed (using the FFT algorithm), multiplied by the impedance and transformed back to yield V_b before the energy kick can be applied to the particles. Note that in the above difference equation, V_b is a function of the phase offset within the bunch. The space charge impedance is computed using

$$Z(\omega) = -j\frac{Z_0}{2\pi}\frac{\omega C}{(\gamma^2 - 1)c}\ln\left[\frac{r_a}{1.06\sigma_\perp}\right] \quad (1)$$

where Z_0 is the vacuum impedance, C is the circumference r_a is the aperture radius and $\sigma_\perp$ is the transverse beam size.

At zero current, the rf phase required to preserve synchronism during acceleration can be computed exactly using the relation

$$\phi_s = \arcsin(V_{acc}/V_{rf}) \quad (2)$$

where V_{acc} is the voltage gain required to preserve sychronism and V_{rf} is the cavity voltage. Because of the losses in the laminations, the accelerating phase must undergo an intensity dependent shift to compensate for the decelerating voltage. During the adiabatic portion of the accelerating cycle, this shift automatically takes place. This is not true in the transition region, where synchrotron motion parameter changes are not adiabatic. For simulation purposes, the phase program is constructed by first setting the accelerating phase to measured values within the transition region. The ideal zero current phase curve is then adapted so as to connect smoothly on both sides of this region. This strategy ensures that the phase jump from ϕ_s to $\pi - \phi_s$ necessary to preserve phase stability at transition has the correct amplitude. Two numerical feedback loops are implemented. The first one is a radial position feedback that is helpful to maintain the beam at the measured momentum offset and phase. The second is a quadrupole motion damper that mimics the one used in operations.

Results

An initial beam distribution uniform in phase and Gaussian in momentum deviation is assumed. The rms width of the momentum distribution is adjusted so as to match the measured bunch length at injection after capture. Approximately 50k particles are tracked. Figure 4 shows the phase and momentum offset predicted both by simulations and beam measurements; the agreement is quite good. Figure 5 shows the rms emittance evolution during the cycle. As expected, the emittance exhibits a sudden jump at transition. Subsequent growth arises because of the complex filamented structure of phase space, still clearly visible in the final phase space distribution. While the increase in core (rms) emittance is on the order of 30%, the full (100%) emittance increases by a factor 2.76. This factor is consistent with an observed factor sightly higher than 2. The simulations predict a 1% particle loss during adiabatic capture and no loss at transition. In operations no losses are observed at transition or as a result of the capture process. The capture loss observed in simulation is understood to be the result of a simplification in the model.

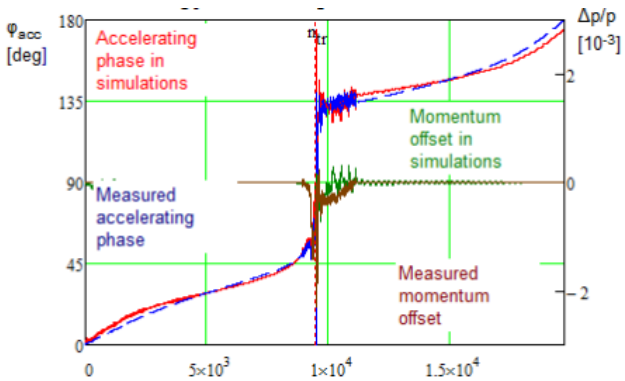

Figure 4: Comparison of the simulated phase and momentum centroids to measured values during a machine cycle.

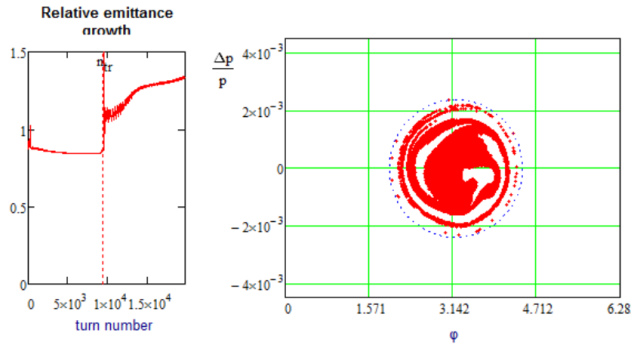

Figure 5: RMS emittance evolution (left) during the cycle and final phase space distribution for current operating conditions.

Figure 6 shows a preliminary result for full PIP-II era. The rf program has been sightly modified. While the core emittance increase remains essentially the same, the increase in total emittance is substantial, going from the previous factor of 2.7 to about 4.

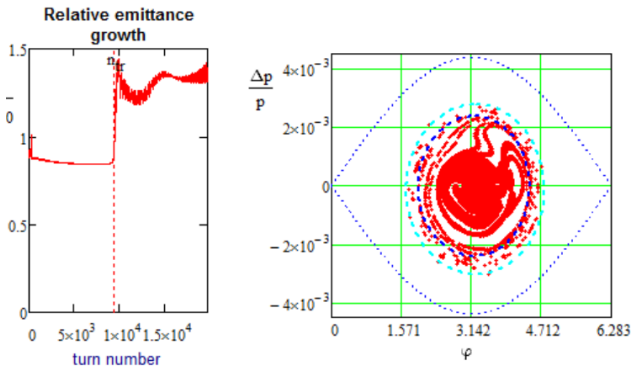

Figure 6: Projected RMS emittance evolution (left) and phase space at the end of the acceleration cycle for PIP-II intensity.

CONCLUSION

Our initial simulations demonstrate reasonable agreement with many qualitative and quantitative aspects of the Booster operational performance. Preliminary results suggest that while a 50% increase in intensity over present level may not substantially degrade the core longitudinal emittance, the increase in full emittance is likely to be more pronounced. We plan to investigate possible additional measures to reduce the emittance blowup. This might include better optimization of the rf voltage program and/or of the timing of the transition phase jump. While a dedicated γ_t jump system is not an option being considered, it may be possible to pulse existing quadrupole correctors to achieve a similar effect, albeit in a less effective way.

ACKNOWLEDGEMENT

The authors wish to thank the Booster Department and the Operations Group for their support in acquiring machine data.

ISBN 978-3-95450-147-2

REFERENCES

[1] V. Lebedev (Ed.), "The PIP-II Reference Design Report", https://indico.fnal.gov/getFile.py/access?resId=0&materialId=2&confId=9939, June 2015

[2] J. Crisp and B. Fellenz, "Fermilab-TM-2145", March 22, 2001.

[3] A. Burov and V. Lebedev, "Impedances of laminated vacuum chambers", http://arxiv.org/pdf/1209.2996.pdf

[4] A. Macridin et al., "Coupling impedance and wake functions for laminated structures with an application to the Fermilab Booster", Phys. Rev. ST Accel. Beams 14, 061003A, June 2011